Available online at www.sciencedirect.com
SCIENCE DIRECT®
Organic Electronics 4 (2003) 155–164
Organic Electronics
www.elsevier.com/locate/orgel

Current status of electrophosphorescent device stability

Raymond C. Kwong *, Michael S. Weaver, Min-Hao Michael Lu, Yeh-Jiun Tung, Anna B. Chwang, Theodore X. Zhou, Michael Hack, Julie J. Brown

Universal Display Corporation, Ewing, NJ 08618, USA

Abstract

Operational stabilities of high-efficiency green and red electrophosphorescent bottom-emission devices with various emitting dopants have been studied. Operational lifetimes of 10,000 h or more, operated at an initial brightness of 600 and 300 cd/m^2 for green and red, respectively, are reported. Operational stabilities of top-emission electrophosphorescent devices and electrophosphorescent devices built on barrier-coated plastic substrates have also been studied and show lifetimes >5000 and >2000 h, respectively, under display level brightness conditions.

Keywords: High-efficiency; Electrophosphorescent; Stability; Lifetime; Top emission; Plastic

1. Introduction

During the past few years, phosphorescent organic light emitting diodes (PHOLED™) based on heavy metal organometallic complexes as dopants have shown rapid developments. The record high efficiencies of this class of OLEDs have attracted a tremendous amount of attention. Since the first report by Baldo and co-workers of efficient PHOLEDs based on platinum porphyrins [1–3], a large number of research articles and presentations have been reported, including both small molecule and polymer systems [4–29]. While the majority of these articles and presentations report outstanding efficiencies, either with new materials (emitting, transporting or blocking) or novel device architectures, a very limited amount of them discuss the topic of operational stabilities [30–33]. Studying the stability of PHOLEDs, as in any OLED device, is crucial in fully understanding the operational principles and degradation mechanisms. This understanding will enable improvements and lead to commercialization of PHOLED technology for application in flat panel display products such as cell phones, and eventually in monitors and televisions. Our group has recently reported highly efficient and stable PHOLEDs [34]. The demonstration of high-efficiency PHOLEDs with long operational lifetimes by our group and others [30–34] has disproved the speculation that PHOLEDs, due to the long exciton lifetimes of the phosphorescent emitters, are more susceptible to degradation than singlet emitter OLEDs. It has been shown that PHOLEDs can be at least as stable as fluorescent devices. Furthermore, the higher efficiency afforded by PHOLEDs, as compared to fluorescent emitting OLEDs, reduces the

* Corresponding author.
E-mail address: rkwong@universaldisplay.com (R.C. Kwong).

1566-1199/$ - see front matter
doi:10.1016/j.orgel.2003.08.012

drive current required to achieve a certain brightness which may translate into higher operational stabilities in PHOLEDs. In this article, we will update the status of our continuing effort in improving the efficiency and stability in a variety of PHOLED products, i.e., bottom-emission PHOLEDs on glass substrates, transparent/top-emission PHOLEDs on glass substrates (TOLEDs™), and bottom-emission PHOLEDs on flexible plastic substrates.

All devices were fabricated by high vacuum ($<10^{-7}$ Torr) thermal evaporation. For the PHOLEDs described in this paper that emit from the substrate surface (referred to as bottom-emission PHOLEDs), the anode electrode is ~1200 Å of indium tin oxide (ITO). For the top-emission PHOLEDs, the anode is comprised of a reflective stack of 160 Å ITO on silver (Ag) with a glass substrate. The organic stack is comprised of 100–200 Å thick of copper phthalocyanine (CuPc) as the hole injection layer (HIL), 300–500 Å of 4,4′-bis[*N*-(1-naphthyl)-*N*-phenylamino]biphenyl (α-NPD) as the hole transporting layer (HTL), 300 Å of 4,4′-bis(*N*-carbazolyl)biphenyl (CBP) doped with 4–12 wt.% of the phosphorescent emitter as the emissive layer (EML), 100–150 Å of aluminum(III)bis(2-methyl-8-quinolinato)4-phenylphenolate (BAlq) as the EML–ETL interface layer, and 300–500 Å of tris(8-hydroxyquinolinato)aluminum (Alq_3) as the electron transporting layer (ETL). The cathode consisted of 10 Å of LiF followed by 1000 Å of Al for bottom-emission devices. The cathode for the top-emitting PHOLEDs consisted of 200 Å Ca deposited by vacuum thermal evaporation, followed by 800 Å ITO by sputter deposition [35]. For the transparent PHOLEDs, a compound cathode of 100 Å of MgAg (10:1 weight ratio of Mg to Ag) followed by 800 Å of sputtered ITO was used. The active area of all the devices was 5 mm^2. All devices, unless otherwise noted, were encapsulated with a glass lid sealed with an epoxy resin in a nitrogen glove box (<1 ppm of H_2O and O_2) immediately after fabrication, and a moisture getter was incorporated inside the package.

The reflectivities and transmissivities of various anodes and cathodes were measured with a Varian Cary 100 UV–Vis spectrophotometer. The electroluminescence was measured with a Photoresearch PR705 spectrophotometer, and the *J–V–L* characteristics were measured with a Keithley 236 source measure unit and a calibrated Si photodiode. Device operational stabilities, measured on several identically fabricated devices, were determined to be within ±5%. All lifetests were conducted in continuous DC drive at room temperature without any initial burn-in periods. Half-life, $T_{1/2}$, is defined as the time for the luminance to decay to 50% of the initial luminance (i.e., $0.5L_0$).

2. Bottom-emission PHOLEDs on glass substrates

Green PHOLEDs based on *fac*-tris(2-phenylpyridine)iridium [$Ir(ppy)_3$] as the phosphorescent dopant have been reported to give a $T_{1/2}$ of 10,000 h at $L_0 = 500$ cd/m^2 [34]. In our recent effort to optimize the device, the stability of the $Ir(ppy)_3$ devices projects to $T_{1/2} \sim 10,000$ h at $L_0 = 600$ cd/m^2 Fig. 1). The initial luminous efficiency (LE) was 23.0 cd/A, corresponding to an external quantum efficiency (η_{ext}) of 6.5%. The drive current density of this device was 2.62 mA/cm^2 at an initial voltage of 7.6 V. After 1000 and 5000 h of operation, the device luminance dropped to 88.2% and 67.4% of the initial value respectively. The CIE coordinate of the device

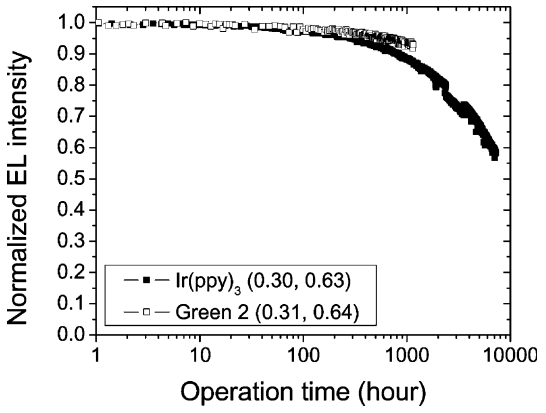

Fig. 1. Lifetime of the $Ir(ppy)_3$ and Green 2 PHOLEDs at $L_0 = 600$ cd/m^2. The CIE coordinates of each device are in parentheses.

was (0.30, 0.63) and was essentially unchanged during lifetest. Extrapolating the lifetime at $L_0 = 600$ cd/m^2, this Ir(ppy)$_3$ PHOLED has $T_{1/2} \sim 10,000$ h.

In the more recent work on improving the efficiency and stability for green PHOLEDs, we have developed a new material system with essentially the same spectral characteristics of Ir(ppy)$_3$. This new system, Dopant Green 2, has brought further improvement in both efficiency and lifetime in the green PHOLED family. At 600 cd/m^2, the initial efficiency of this green PHOLED device was 29.3 cd/A ($\eta_{ext} = 7.8\%$). The CIE coordinate was (0.31, 0.64), indistinguishable from the Ir(ppy)$_3$ device by the human eye. At the same initial brightness as the Ir(ppy)$_3$ device, i.e. $L_0 = 600$ cd/m^2, it can be seen that the Green 2 device is more stable (Fig. 1). The drive current was 2.05 mA/cm^2 at an initial voltage of 8.0 V. After 1000 h of operation, the luminance dropped to 93.5% of its initial value, compared to 88.2% of the Ir(ppy)$_3$ device. Although it is too early to project $T_{1/2}$ at 1000 h, we expect its $T_{1/2}$ to be ~15,000 h.

Due to the low photopic response of the human eye to red, and the relatively large contribution of the red in brightness for a balanced white color, the red component constitutes a large portion of the total power consumption for a full color display. It is therefore critical to develop highly efficient red devices with high stabilities. A 17.6 cd/A orange–red PHOLED based on iridium(III)bis(2-phenylquinolyl-N,$C^{2'}$)acetylacetonate[PQ$_2$Ir(acac)] as the phosphorescent emitter has been reported to have a $T_{1/2} \sim 5000$ h at $L_0 = 300$ cd/m^2 [34]. We report here more recent results on red PHOLEDs using dopants Red 1, Red 2 and Red 3 [36].

The efficiencies of red PHOLEDs are very high. The CIE coordinates, independent of current density, are (0.61, 0.38), (0.61, 0.39) and (0.65, 0.35) respectively. Obviously, Red 1 and Red 2 are orange–red, and Red 3 is red emitting. In Fig. 2, the luminous efficiency is plotted against the luminance for the different devices. The efficiencies do not suffer from significant roll-off as observed in some platinum porphyrin red devices. One explanation is the shorter triplet exciton lifetime of the new red phosphorescent dopants (typically <5 μs), leading to reduced triplet–triplet exciton annihilation, compared to platinum porphyrins

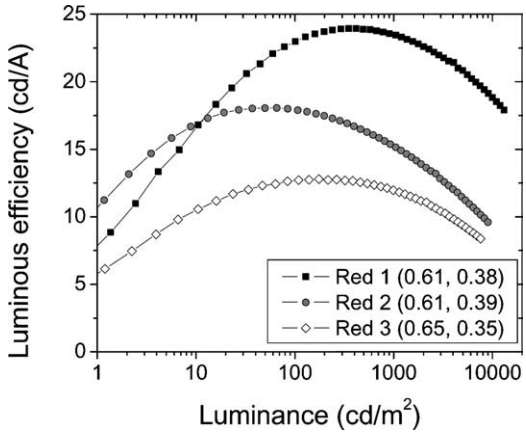

Fig. 2. Luminous efficiency versus luminance of the Red 1, Red 2 and Red 3 PHOLEDs. The CIE coordinates of each device are in parentheses.

(typically >30 μs)[3]. But more importantly, the overall device composition such as the type and thickness of the charge transporting materials, electrode materials, emitter doping concentrations, etc., critically affects the efficiency roll-off, not just the exciton lifetime alone. This hypothesis is well supported by the fact that certain fluorescent small molecule and polymer OLEDs, with very short-lived singlet exciton (typically <10 ns), show the same degree of, or even higher, efficiency roll-off compared to phosphorescent OLEDs [37]. The maximum efficiencies of the Red 1, Red 2 and Red 3 device are 23.9 cd/A at 410 cd/m^2, 18.1 cd/A at 66 cd/m^2, and 12.8 cd/A at 175 cd/m^2, respectively. At 300 cd/m^2, a typical display brightness for the red component in full color displays, the efficiencies are 23.9, 17.0 and 12.7 cd/A, respectively. Even at 10,000 cd/m^2, high efficiencies of 18.6, 9.3, and 8.0 cd/A are retained. The performance is summarized in Table 1. The external quantum efficiencies are greater than 10%. The relatively lower luminous efficiency of the Red 3 device is only due to the deeper red color compared to the orange–red color of the Red 1 and Red 2 devices. The outstanding performance at both low and high current drives enables their use in both active and passive modes in displays.

The operational stability of the red devices is very high. The initial luminance for stability testing was selected to be 300 cd/m^2 for all three

Table 1
Performance summary of the Red 1, Red 2 and Red 3 PHOLEDs (efficiency and lifetime are recorded at $L_0 = 300$ cd/m^2)

PHOLED	CIE	η_{ext} (%)	LE (cd/A)	% Retained at 1000 h
Red 1	0.61, 0.38	13.6	23.9	92.5
Red 2	0.61, 0.39	10.6	16.7	94.5
Red 3	0.65, 0.35	11.3	12.7	93.5

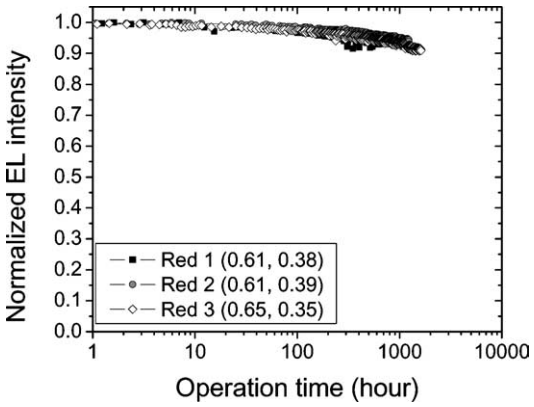

Fig. 3. Lifetime of the Red 1, Red 2 and Red 3 PHOLEDs at $L_0 = 300$ cd/m^2. The CIE coordinates of each device are in parentheses.

devices. In Fig. 3, the normalized luminance is plotted against the operational time. The drive current was respectively 1.26, 1.80 and 2.36 mA/cm^2 at initial voltages of 8.8, 8.5 and 7.9 V for the Red 1, Red 2 and Red 3 devices. After 1000 h of continuous operation, the luminance was retained respectively at 92.5%, 94.5% and 93.5%. Again, the exact projection of the half-life at this point is difficult, however, in our experience, based on these lifetime trends, $T_{1/2} > 15,000$ h is expected.

3. Transparent/top-emitting PHOLEDs on glass substrates

Conventional OLEDs employ a bottom-emitting structure where the cathode is a reflective metal, the anode is a transparent ITO anode, and light is emitted through the anode and the glass substrate (Fig. 4(a)). While this represents the most mature OLED technology, alternative electrode configurations are possible. Top-emitting

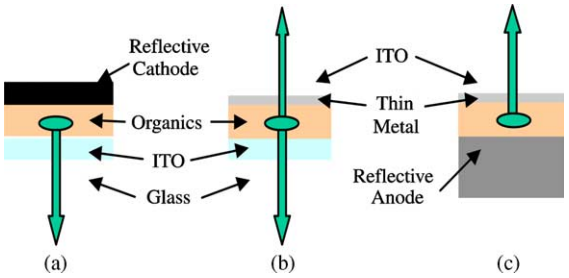

Fig. 4. (a) Conventional OLED with ITO/glass anode and reflective cathode; (b) transparent OLED with ITO/glass anode and thin metal/ITO compound cathode; and (c) top-emitting OLED with reflective anode and thin metal/ITO compound cathode.

OLEDs, with an opaque/reflective bottom anode and a transparent top cathode (Fig. 4(b)) have been demonstrated by Bulovic et al. in 1997 [38]. Top-emitting OLEDs are well suited in high-resolution active-matrix OLED displays where they are deposited over a planarized back-plane, thus increasing the aperture ratio over displays employing bottom-emitting OLEDs [39]. Recently, our group has demonstrated that top-emitting OLEDs can be more efficient than corresponding bottom-emitting OLEDs due to favorable microcavity effects [39]. Another possibility is to use a transparent cathode in conjunction with an ITO anode to make a fully transparent device (Fig. 4(c)) with obvious applications in see-through displays, etc. [40]. In this section, we will review recent progress in top-emitting and transparent OLEDs which are enabled by the same transparent cathode technology.

All devices in this section used the Ir(ppy)$_3$ PHOLED standard structure. The emission intensity of top-emitting OLEDs depends strongly on the top ITO layer thickness due to microcavity effects. Both experimental data and modeling indicate that 800 Å is the optimal ITO thickness for

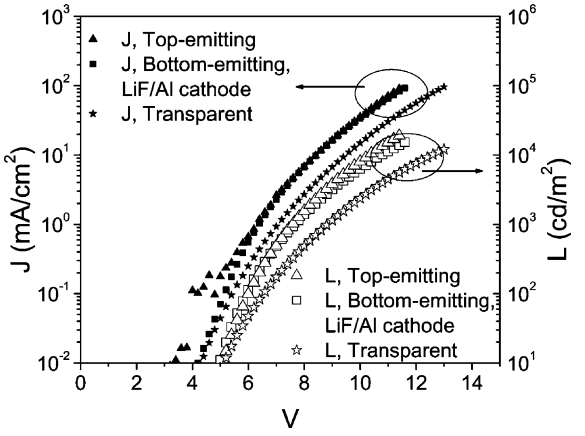

Fig. 5. J–V–L curve of a top-emitting OLED compared with that of a bottom-emitting OLED. The luminance of the top-emitting OLED is measured through the cover glass.

these green phosphorescent top-emitting OLEDs [39]. The J–V–L characteristics of the top and bottom-emitting OLEDs are plotted in Fig. 5. The J–V curves of the top and bottom-emission OLEDs are identical within measurement uncertainties, while the top-emission OLED has a slightly higher luminous efficiency. At 10 mA/cm^2 the luminance efficiency is 20.3 cd/A for the bottom emission and 23.1 cd/A for the top-emission OLED (through the cover glass), i.e. 15% higher. The transmissivity of glass/Ca (200 Å)/ITO (800 Å) is 62.8% at $\lambda = 515$ nm [$\sim$ the peak of Ir(ppy)$_3$ emission], much less than the transmissivity of 89.9% for the ITO coated glass. The reflectivity of the Ag/ITO anodes is 85.5% at $\lambda = 515$ nm, again less than that of the Al cathodes at 88.5%. Overall, the electrodes of the bottom-emission OLEDs are more reflective/transmissive than those of the top-emission ones. Therefore, the enhanced luminance in top-emission OLEDs can only be attributed to the more favorable microcavity structure.

The J–V–L curve of the transparent OLED is also shown in Fig. 5. The current density at a given bias voltage is lower than that of the top and bottom-emission OLED because of the slightly thicker organic layer used and the lower electron injection from the MgAg/ITO cathode. At 10 mA/cm^2, the luminance efficiency is 16.4 cd/A which is based on the sum of the emission from both sides. Approximately 75% of the light is emitted through the ITO anode. The luminance efficiency is lower due to the low transmission of the MgAg/ITO cathode (55% at 515 nm).

The far-field photon radiation from these devices was measured directly with a Photoresearch PR705 spectrophotometer. Due to the relative size of the devices and the focal spot of the spectrophotometer this measurement could be carried out reliably only up to a far-field angle of 60° from normal. Fig. 6 shows the angular dependence of photon radiation for the top-emitting OLED (through the cover glass), the same top-emitting OLED corrected for the cover glass, and the corresponding bottom-emitting OLED. In accordance with our predictions, photon radiation is higher in these top-emitting OLEDs even uncorrected for the cover glass. There is only a weak angular dependence which indicates that the emission is approximately Lambertian in this angular range. Estimating the integrated photon flux by the formula $\sum I(\theta)\sin(\theta)\Delta\theta$, where $I(\theta)$ is the photon radiation at angle θ, the uncorrected and corrected top-emission devices were found to emit 4.2% and 20.8% more photons than the bottom-emission OLED in the forward 120° cone, respectively.

Fig. 7 shows DC life-testing results of a typical long-lived bottom-emitting OLED and a transparent OLED with a MgAg/ITO based compound cathode. The initial luminance is 600 cd/m^2 for both devices. For the transparent OLED, it is the

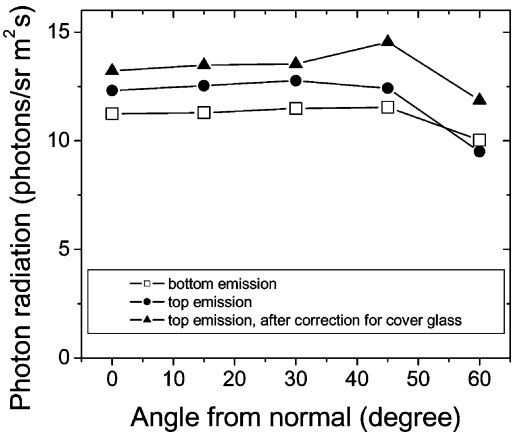

Fig. 6. Photon radiation versus far-field angle, all data was taken at $J = 10$ mA/cm^2.

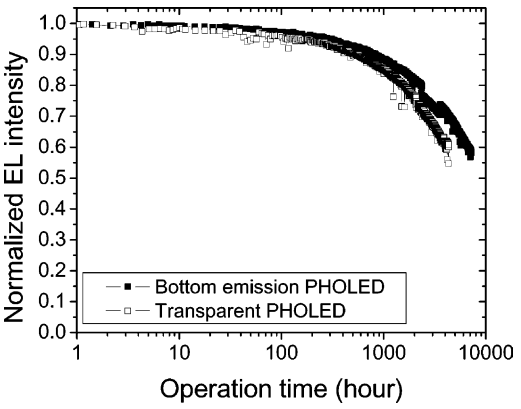

Fig. 7. Lifetime of a bottom-emitting $Ir(ppy)_3$ PHOLED and a transparent $Ir(ppy)_3$ PHOLED with MgAg/ITO cathode.

sum of the emission from both sides. The current density through the transparent OLED is slightly higher due to the lower external efficiency because of the absorption in the MgAg layer. The bottom-emitting OLED has a half-life of ~10,000 h, and the transparent OLED is projected to reach over 6000 h. The luminance degradation is observed to be coulombic, i.e., solely dependant upon the aggregate charge flowing through the device ($J_{OLED}T_{1/2OLED} \approx J_{TOLED}T_{1/2TOLED} \approx$ constant). This has been reported by other groups [41] and indicates the absence of extrinsic decay mechanisms such as dark-spot formation.

4. Bottom-emission PHOLEDs on flexible plastic substrates

Glass substrates do not allow exploitation of the flexibility of both polymeric [42] and small molecule [43,44] OLEDs to enable new light weight, rugged, flexible displays [45] produced by roll to roll manufacturing. Plastic substrates, however, do allow for such displays. Fig. 8 shows examples of PHOLEDs grown on flexible substrates. Although flexible OLED (FOLED™) displays on a plastic substrate have been demonstrated [45], conventional encapsulation techniques are ineffective due to moisture permeation through the substrate and long lifetimes had not been shown until recently [46]. To enable a device lifetime of 10,000 h, the maximum permeability of a substrate to the ingress of water can be estimated within an order of magnitude to be 5×10^{-6} g/m^2/day [47]. This is an *estimated upper limit* on the requirement for the substrate and does not take into account any degradation processes at the anode/organic interface or within the organic materials themselves that may be catalyzed by water [48]. Typically, plastic materials have a water vapor permeation rate of 10^{1}–10^{-1} g/m^2/day at 25 °C and are therefore inadequate for OLEDs. Furthermore, a leak rate below 10^{-2} g/m^2/day is difficult to achieve using inorganic barrier layers deposited at or near room temperature, due to pinholes and defects. The high surface roughness of commercially available plastic substrates exacerbates these problems [49,50].

Here we present PHOLEDs with extended operating lifetimes using a hybrid organic–inorganic multilayer barrier coating [47,51] on 175-μm-thick heat stabilized polyethylene terephthalate (PET), demonstrating that suitably processed plastic substrates can be used to fabricate long-lived OLEDs. The composite barrier consists of alternating layers of polyacrylate films and an inorganic oxide. By repeating the alternating films, the polymer layers 'decouple' any defects in the oxide layers. This prevents the propagation of defects through the multilayer structure. The optical and barrier properties of the composite substrate can be tailored by varying the total number and thickness of the polymer and inorganic layers in the thin-film coating, yielding an engineered flexible substrate [52]. The barrier-coated PET substrates exhibit moisture barrier performance below the limit of MOCON [53] detection instruments (5×10^{-3} g/m^2/day). More detailed measurements of permeability based on the corrosion of Ca are published elsewhere [54] and indicate a permeation rate through the substrate and barriers estimated to be 4×10^{-6} g/m^2/day.

PHOLEDs were fabricated on the barrier-coated flexible substrates to test the viability of using them to make long-lived flexible displays. Onto the barrier were grown sequentially deposited layers of patterned indium tin oxide (ITO) [160 nm] as the anode contact. All materials and fabrication steps were identical to the $Ir(ppy)_3$ based PHOLED described in the previous section.

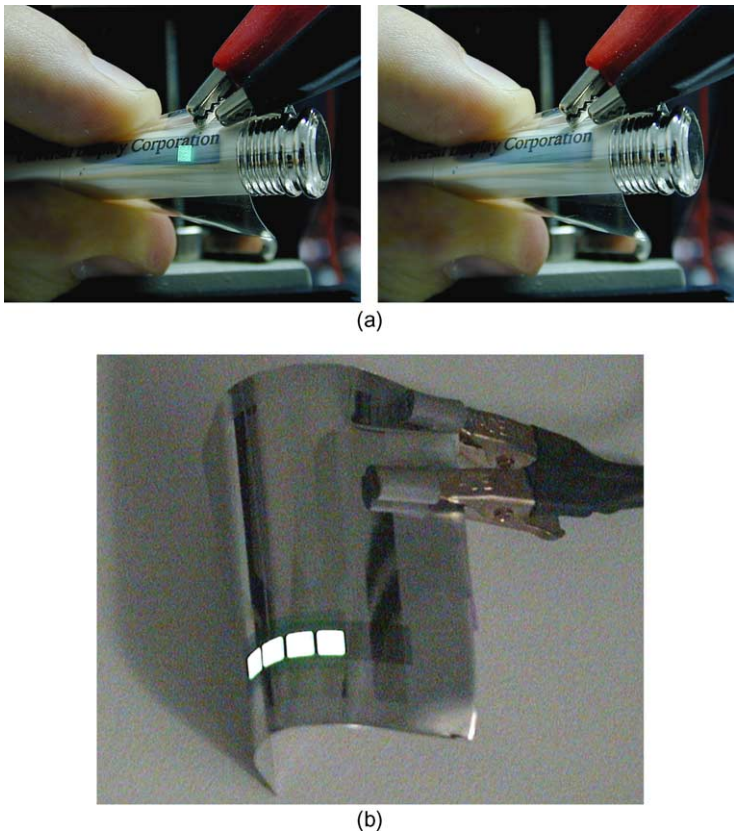

Fig. 8. Examples of OLEDs fabricated on flexible substrates. (a) A flexible transparent OLED pixel is shown here, wrapped around a pen, in both its on and off states. The substrate is 0.175 mm thick heat stabilized PET, the pixel is 5 mm^2 in area and the radius of curvature is 5 mm. (b) A TOLED pixel fabricated on a 0.125 mm thick metal foil. The pixels have an active area of 5 mm^2.

The FOLED had a peak luminous efficiency of 17.5 cd/A ($\eta_{ext} = 4.8\%$) at 600 cd/m^2. This is slightly lower than the same device on glass, primarily because of the lower transparency and light outcoupling efficiency due to the thicker ITO and the multilayer barrier coating on the plastic substrate. (Note: more recently, the barrier-coated substrates have been further optimized to enable better light outcoupling from the substrate, and plastic substrate devices have shown efficiency comparable to that of glass substrate devices [55].) The lifetime was measured at an initial luminance of 425 cd/m^2 at a current density of 2.5 mA/cm^2. Fig. 9 shows a typical plot of normalized luminance versus time for this device. A device fabricated on glass with the same organic and metal layers as the FOLED and encapsulated using the same procedures (i.e., with glass lid) is also shown for comparison. It was driven at 2.6 mA/cm^2 ($L_0 = 600$ cd/m^2). After a brief initial rise in luminance during the first 24 h of testing, the FOLED decays to 50% of its initial luminance in 3800 h, as compared to 10,000 h for equivalent devices made on glass [34]. At 3800 h the PHOLED on glass is at 69% of its initial luminance. Assuming lifetime is inversely proportional to drive current [34], these results correspond to a lifetime of 16,000 h at 100 cd/m^2 for the encapsulated plastic device. The shorter lifetime for the devices on the barrier-coated plastic substrate may be partly due to the superior barrier properties of the glass substrates. However, we note that the epoxy exhibited poorer adhesion to the barrier-coated plastic than to the glass; indeed, after

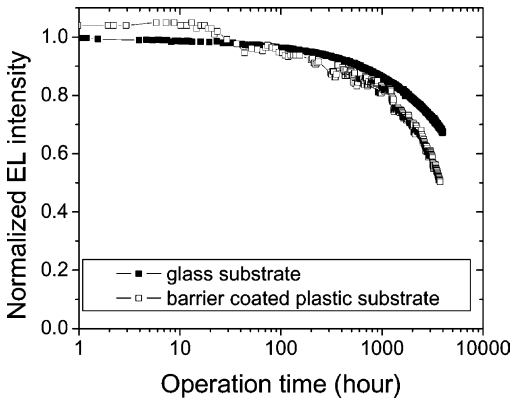

Fig. 9. Lifetime of an $Ir(ppy)_3$ PHOLED on barrier-coated PET driven at 2.5 mA/cm^2. A PHOLED with the same architecture on ITO coated glass is shown for comparison driven at 2.6 mA/cm^2.

~3000 h a high failure rate of the plastic package due to delamination of the lid was observed. Faster diffusion of moisture through the edge seal of the flexible plastic versus glass substrate could therefore contribute to the lifetime enhancement of the glass-based pixels.

The same type of multilayer barrier structure used on the PET substrate can also be applied over the PHOLED as a hermetic encapsulant [55]. In this truly flexible (substrate and encapsulation) configuration, the PHOLED is protected on all sides from moisture ingress. Furthermore, no edge seal or glass/metal lid is required, reducing package volume and materials cost. Preliminary results indicate that the lifetime of FOLEDs encapsulated using a multilayer barrier structure approaches that of similarly encapsulated PHOLEDs on glass [55].

5. Summary

Efficient and stable bottom/top-emission and flexible PHOLEDs have been demonstrated. Enabled by new phosphorescent materials, bottom emission, long-lived green PHOLEDs showed efficiencies of >29 cd/A. Two orange–red and one red devices showed efficiencies of 23.9, 17.0 and 12.7 cd/A respectively. All these devices have lifetimes predicted to be >15,000 h at display brightness. Even at higher brightness, these devices retain very high efficiencies, thus suiting not only active matrix but also passive matrix display operations.

We demonstrated that top-emitting OLEDs employing identical organic layers can be more efficient than conventional bottom-emitting devices due to favorable microcavity effects. Top-emitting OLEDs based on Ag/ITO anodes and Ca/ITO transparent compound cathodes emit 20.8% more photons in the forward 120° cone than corresponding bottom-emitting OLEDs. We also fabricated long-lived transparent OLEDs with MgAg/ITO cathodes which proved that the lifetime is not limited by the sputter deposition of ITO. We expect both types of OLEDs to enable a new generation of displays.

For devices on plastic substrates, in order to realize the barrier properties necessary to prevent degradation of FOLEDs, a novel non-conformal multilayered film was used that reduces the permeation rate of water vapor through a flexible substrate to less than 2×10^{-6} g/m^2/day. Based on measurements of an epoxy sealed PHOLED package with a barrier-coated PET substrate and glass lid, a $T_{1/2}$ of 3800 h from an initial luminance of 425 cd/m^2 was observed. We also demonstrated a 240×64 80 dpi passive matrix PHOLED display fabricated on a similarly barrier-coated PET substrate (Fig. 10). Combined with a conformal encapsulation or lamination technology, which could be based on the same hybrid multilayer stack [55],

Fig. 10. A video rate 240×64 80 dpi passive matrix monochrome green PHOLED display fabricated on a barrier-coated 175-μm-thick PET substrate.

our results represent a critical first step in the realization of plastic-based OLEDs for flexible displays.

Acknowledgements

This work is partially funded by the Defense Advanced Research Projects Agency. The authors are grateful to Professors Stephen R. Forrest and Mark E. Thompson for their numerous innovations and long standing support of this work. Furthermore, the authors thank Prof. Thompson and his group at the University of Southern California, and PPG Industries for their work on new materials; Vitex Systems, and Pacific Northwest National Laboratory for their work on barrier-coated plastics; and Prof. Forrest and his group at Princeton University, and Prof. C. Adachi of Chitose Institute of Science and Technology for helpful discussions.

References

[1] M.A. Baldo, D.F. O'Brien, Y. You, A. Shoustikov, S. Sibley, M.E. Thompson, S.R. Forrest, Nature 395 (1998) 151.
[2] D.F. O'Brien, M.A. Baldo, M.E. Thompson, S.R. Forrest, Appl. Phys. Lett. 74 (1999) 442.
[3] R.C. Kwong, S. Sibley, T. Dubovoy, M. Baldo, S.R. Forrest, M.E. Thompson, Chem. Mater. 11 (1999) 3709.
[4] C. Adachi, M.A. Baldo, S.R. Forrest, M.E. Thompson, Appl. Phys. Lett. 77 (2000) 904.
[5] M.A. Baldo, S. Lemansky, P.E. Burrows, M.E. Thompson, S.R. Forrest, Appl. Phys. Lett. 75 (1999) 4.
[6] R.C. Kwong, S. Lemansky, M.E. Thompson, Adv. Mater. 11 (2000) 1134.
[7] T. Guo, S. Chang, Y. Yang, R.C. Kwong, M.E. Thompson, Org. Electron. 1 (2000) 15.
[8] C. Adachi, M.A. Baldo, S.R. Forrest, S. Lamansky, M.E. Thompson, R.C. Kwong, Appl. Phys. Lett. 78 (2001) 1622.
[9] S. Lemansky, P. Djurovich, D. Murphy, F. Abdel-Razzaq, H.-E. Lee, C. Adachi, P.E. Burrows, S.R. Forrest, M.E. Thompson, J. Am. Chem. Soc. 123 (2001) 4304.
[10] S. Lamansky, R.C. Kwong, M. Nugent, P.I. Djurovich, M.E. Thompson, Org. Electron. 2 (2001) 53.
[11] C. Adachi, R.C. Kwong, P. Djurovich, V. Adamovich, M.A. Baldo, M.E. Thompson, S.R. Forrest, Appl. Phys. Lett. 79 (2001) 2082.
[12] H.Z. Xie, M.W. Liu, O.Y. Wang, X.H. Zhang, C.S. Lee, L.S. Hung, S.T. Lee, P.F. Teng, H.L. Kwong, H. Zheng, C.M. Che, Adv. Mater. 13 (2001) 1245.
[13] M. Ikai, S. Tokito, Y. Sakamoto, T. Suzuki, Y. Taga, Appl. Phys. Lett. 79 (2001) 156.
[14] Y. Wang, N. Herron, V.V. Grushin, D. LeCloux, V. Petrov, Appl. Phys. Lett. 79 (2001) 449.
[15] C.-L. Lee, K.B. Lee, J.-J. Kim, Appl. Phys. Lett. 77 (2000) 2280.
[16] J.P.J. Markham, T. Anthopoulos, S.W. Magennis, I.D.W. Samuel, N.H. Male, O. Salata, SID Dig. (2002) 1032.
[17] S.-C. Lo, N.A.H. Male, J.P.J. Markham, S.W. Magennis, P.L. Burn, Q.V. Salata, I.D.W. Samuel, Adv. Mater 14 (2002) 975.
[18] J.P.J. Markham, S.-C. Lo, P.L. Burn, I.D.W. Samuel, Appl. Phys. Lett. 80 (2002) 2645.
[19] X. Zhou, D.S. Qin, M. Pfeiffer, J. Blochwitz-Nimoth, A. Werner, J. Drechsel, B. Maennig, K. Leo, M. Bold, P. Erk, H. Hartmann, Appl. Phys. Lett. 81 (2002) 4070.
[20] X. Gong, M.R. Robinson, J.C. Ostrowski, D. Moses, G.C. Bazan, A.J. Heeger, Adv. Mater. 14 (2002) 581.
[21] K.M. Tang, C.W. Tang, Appl. Phys. Lett. 92 (2002) 3447.
[22] C. Adachi, M.A. Baldo, M.E. Thompson, S.R. Forrest, J. Appl. Phys. 90 (2001) 5048.
[23] W. Zhu, Y. Mo, M. Yuan, W. Yang, Y. Cao, Appl. Phys. Lett. 80 (2002) 2045.
[24] X. Chen, J.-L. Liao, Y. Liang, M.O. Ahmed, H.-E. Tseng, S.-A. Chen, J. Am. Chem. Soc. 125 (2003) 636.
[25] X. Gong, J.C. Ostrowski, G.C. Bazan, D. Moses, A.J. Heeger, M.S. Liu, A.K.-Y. Jen, Adv. Mater. 15 (2003) 45.
[26] X. Jiang, A.K.-Y. Jen, B. Carlson, L.R. Dalton, Appl. Phys. Lett. 80 (2002) 713.
[27] X. Gong, J.C. Ostrowski, G.C. Bazan, D. Moses, A.J. Heeger, Appl. Phys. Lett. 81 (2002) 3711.
[28] G.E. Jabbour, J.-F. Wang, N. Peyghambarian, Appl. Phys. Lett. 80 (2002) 2026.
[29] S. Okada, H. Iwawaki, M. Furugori, J. Kamatani, S. Igawa, T. Moriyama, S. Miura, A. Tsuboyama, T. Takiguchi, H. Mizutani, SID Dig. (2002) 1360.
[30] P.E. Burrows, S.R. Forrest, T.X. Zhou, L. Michalski, Appl. Phys. Lett. 76 (2000) 2493.
[31] T. Tsutui, M.J. Yang, M. Yahiro, K. Nakamura, T. Watanabe, T. Tsuji, Y. Fukuda, T. Wakimoto, S. Miyahuchi, Jpn. J. Appl. Phys. 38 (1999) L1502.
[32] T. Watanabe, K. Nakamura, S. Kawami, Y. Fukuda, T. Tsuji, T. Wakimoto, S. Miyaguchi, Proc. SPIE 4105 (2000) 175.
[33] T. Watanabe, K. Nakamura, S. Kawami, Y. Fukuda, T. Tsuji, T. Wakimoto, S. Miyaguchi, M. Yahiro, N.-J. Yang, T. Tsutsui, Synth. Met. 1221 (2001) 203.
[34] R.C. Kwong, M.R. Nugent, L. Michalski, T. Ngo, K. Rajan, Y.-J. Tung, M.S. Weaver, T.X. Zhou, M. Hack, M.E. Thompson, S.R. Forrest, J.J. Brown, Appl. Phys. Lett. 81 (2002) 162.
[35] P.E. Burrows, G. Gu, S.R. Forrest, E.P. Vicenzi, T.X. Zhou, J. Appl. Phys. 87 (2000) 3080.

[36] R.C. Kwong, M.R. Nugent, T. Ngo, K. Rajan, L. Michalski, Y.-J. Tung, J.J. Brown, in: Proceedings of the 21st International Display Research Conference in Conjunction with the 8th International Display Workshops, 2001, p. 1774.
[37] R.C. Kwong, M.R. Nugent, L. Michalski, T. Ngo, K. Rajan, Y.-J. Tung, M.S. Weaver, T.X. Zhou, M. Hack, J.J. Brown, SID Dig. (2002) 1365.
[38] (a) V. Bulovic, P. Tian, P.E. Burrows, M.R. Gokhale, S.R. Forrest, Appl. Phys. Lett. 70 (1997) 2954;
(b) V. Bulovic, P. Tian, P.E. Burrows, M.R. Gokhale, S.R. Forrest, US Patent Nos. 5,703,436 and 5,707,745.
[39] M.-H. Lu, M.S. Weaver, T.X. Zhou, M. Rothman, R.C. Kwong, M. Hack, J.J. Brown, Appl. Phys. Lett. 81 (2002) 3921.
[40] V. Bulovic, G. Gu, P.E. Burrows, M.E. Thompson, S.R. Forrest, Nature 380 (1996) 29.
[41] H. Aziz, Z.D. Popovic, N.-X. Hu, Appl. Phys. Lett. 81 (2002) 370.
[42] G. Gustafsson, Y. Cao, G.M. Treacy, F. Klavetter, N. Colaneri, A.J. Heeger, Nature 357 (1992) 477.
[43] G. Gu, P.E. Burrows, S. Venkatesh, S.R. Forrest, Opt. Lett. 22 (1997) 172.
[44] G. Gu, P.E. Burrows, S.R. Forrest, US Patent No. 5,844,363.
[45] M.S. Weaver, J.J. Brown, R.H. Hewitt, S.Y. Mao, L.A. Michalski, T. Ngo, K. Rajan, M.A. Rothman, J.A. Silvernail, W.E. Bennet, C. Bonham, P.E. Burrows, G.L. Graff, M.E. Gross, M. Hall, E. Mast, P.M. Martin, Inform. Display 17 (5–6) (2001) 26.
[46] M.S. Weaver, L.A. Michalski, K. Rajan, M.A. Rothman, J.A. Silvernail, J.J. Brown, P.E. Burrows, G.L. Graff, M.E. Gross, P.M. Martin, M. Hall, E. Mast, C. Bonham, W. Bennett, M. Zumhoff, Appl. Phys. Lett. 81 (2002) 2929.
[47] P.E. Burrows, G.L. Graff, M.E. Gross, P.M. Martin, M. Hall, E. Mast, C. Bonham, W. Bennet, L. Michalski, M.S. Weaver, J.J. Brown, D. Fogarty, L.S. Sapochak, Proc. SPIE 4105 (2000) 75.
[48] F. Papadimitrikopoulus, X.M. Zhang, K.A. Higginson, IEEE J. Sel. Top. Quant. Electron. 4 (1998) 49.
[49] A. Yoshida, A. Sugimoto, T. Miyadera, S. Miyaguchi, J. Photopolym. Sci. Technol. 14 (2) (2001) 327.
[50] H. Chatham, Surf. Coat. Technol. 78 (1996) 1.
[51] J.D. Affinito, M.E. Gross, P.A. Mournier, M.K. Shi, G.L. Graff, J. Vac. Sci. Technol. A 17 (1999) 1974.
[52] Barix™, Vitex Systems Inc., 3047 Orchard Parkway, San Jose, CA 95134, USA.
[53] MOCON 3/31G, Minneapolis, MN 55428, USA.
[54] G. Nisato, P.C.P. Bouten, P.J. Slinkkerveer, W.D. Bennet, G.L. Graff, N. Rutherford, L. Wiese, in: Asia Display/IDW'01 Proc., 2001.
[55] A.B. Chwang, M.A. Rothman, S. Mao, R. Hewitt, M.S. Weaver, J.A. Silvernail, K. Rajan, M. Hack, J.J. Brown, X. Chu, L. Moro, T. Krajewski, N. Rutherford, Appl. Phys. Lett. 83 (2003) 413.